

Slow Electrons from Electron-Impact Ionization of He, Ne, and Ar[†]

J. T. Grissom,* R. N. Compton, and W. R. Garrett

Health Physics Division, Oak Ridge National Laboratory, Oak Ridge, Tennessee 37830

(Received 24 April 1972)

A trapped-electron technique is used to determine the integral cross sections for production of secondary electrons in the energy range from 0 to 1 eV resulting from electron-impact ionization of He, Ne, and Ar. For incident electron energies above 150 eV the slow-electron production cross section decreases approximately as the total-ionization cross section. A simple Born calculation for the case of atomic hydrogen also shows this general behavior. The measured absolute cross sections compare well with recently measured relative angular distributions and with Born and Born-exchange calculations.

I. INTRODUCTION

Electron-impact ionization of atoms and molecules has been the subject of numerous studies since the turn of the century. The noble gases have served as model systems for theory and experiment. Most of the experimental work has been concerned with measurements of total- and partial-ionization cross sections and with the behavior of the cross section with energy at threshold. Until the past few years, these latter measurements have provided the sole basis for comparison with theory. Recently, however, Ehrhardt and his colleagues¹ have made significant advances in the experimental studies of electron-impact ionization by analyzing both the primary and secondary electrons and counting them in coincidence.

Secondary electrons are produced when any type of sufficiently energetic radiation interacts with matter. These secondaries can produce further ionization by creating tertiary electrons and so forth until all of the electrons are below the ionization threshold of the medium. Ultimately the electrons either recombine with the ions produced, attach to molecular constituents of the medium, or come to thermal equilibrium with the medium. The energies of these secondary, tertiary, etc., electrons are, therefore, of considerable interest in radiation chemistry. Recently, Opal, Peterson, and Beaty² reported relative measurements of cross sections which are differential in energy and angle for electrons ejected from helium for incident electron energies between 100 and 2000 eV. The measurements were integrated over angle, and the resulting secondary-electron cross sections were normalized by absolute elastic scattering data to obtain cross-section values. These measurements were the first of their kind and provided a basis for comparison with theoretical calculations of secondary-electron energy distributions. The secondary-electron distributions of Opal, Peterson, and Beaty² extend down to ~ 5 eV where the measurements became difficult. In the present paper

a trapped-electron technique is used to obtain cross sections for the production of secondary electrons in the difficult energy range from 0 to 1 eV.

II. EXPERIMENTAL

The trapped-electron apparatus employed in these studies has been described previously,³ and a complete description of the trapped-electron technique can be found in the original paper of Schulz.⁴ The main experimental innovation in this work is the precise determination of the well depth.

The depth of the potential well in the scattering chamber can be expressed as the sum of two terms,

$$W = \alpha V + W_0, \quad (1)$$

where V is the external potential applied to the collector electrode, W_0 is the contribution to the well depth from surface and contact potentials in the scattering chamber, and α is a constant of proportionality which is a function of the geometry of the grid and collector and must be determined experimentally. The potential W_0 represents a built-in well depth whose magnitude depends only on the composition and condition of the surfaces in the scattering chamber. Gold plating all surfaces helps to minimize the magnitude of W_0 .

The constant α is determined by measuring the energy position of the 19.31-eV He⁻(1s2s²)²S transmission resonance⁵ as a function of the collector voltage V . Since the average energy of the beam in the scattering chamber corresponds to the energy with which the electrons enter the chamber plus W , then changing the well depth by an amount ΔW changes the beam energy by an equal amount and causes a corresponding shift ΔW in the apparent position of the transmission resonance. The method is illustrated in Fig. 1, showing the position of the transmission resonance for three values of the collector voltage V . The coefficient α is given by the ratio $\Delta W/\Delta V$ since W_0 is a constant.

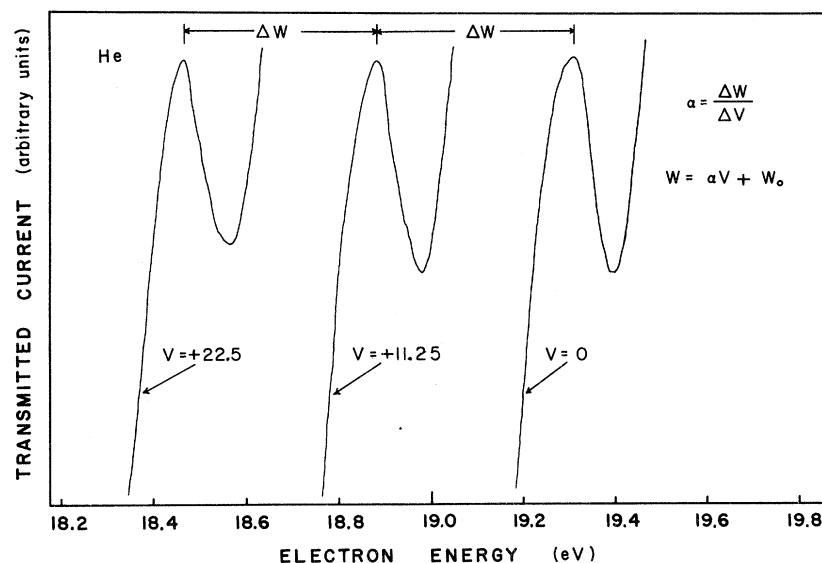


FIG. 1. Position of the 19.31-eV He transmission resonance as a function of the trapped-electron collector potential.

Figure 2 shows a representative plot of the energy shift as a function of V for ten measurements. The value of α is given by the slope of the straight line through the data points. Many measurements led to an average value of $\alpha = 0.0187$.

The coefficient α is dependent only on the geometry of the screening grid and collector electrode in the scattering chamber and does not have to be determined for each gas used in the spectrometer. However, W_0 depends on the surface and contact potentials and consequently it is a function of the gas used. W_0 was measured each time the spectrometer was used, since the surface potentials can vary with changing conditions of the electrode surface.

The simplest method of determining W_0 depends on observing the extinction of the positive-ion current. Since the mass of an electron is more than 10^3 times smaller than the mass of an atom, the positive ions resulting from collisions with electrons are produced with essentially zero kinetic energy. Thus, no positive-ion current will be measured at the collector electrode unless there is a net negative potential along the axis of the scattering chamber where the ions are being formed. Whenever the ion current vanishes, the net potential W along the axis of the scattering chamber is zero. If the collector voltage required to cause the positive-ion current to vanish is designated V_0 , then

$$W = 0 = \alpha V_0 + W_0$$

and W_0 is equal to $-\alpha V_0$.

An alternative method for determining W_0 depends upon a measurement of the increase in the electron-impact excitation cross section above threshold for a specific electronic state of the

atom. Extrapolation of the trapped-electron current versus applied voltage back to zero current in a manner similar to that described above gives W_0 .

The accuracy with which α and W_0 can be measured is comparable. Values of W_0 measured by both of the techniques described above have been found to agree consistently to within 0.01 eV for the noble gases. W_0 itself is usually only 0.02 to 0.05. Consequently, an uncertainty on the order of 0.01 eV can be assigned to the value of W_0 . Repeated measurements of α are consistent to within an uncertainty of 0.01 eV in a well-depth energy of 0.2 eV. Thus, for well depths up to about 0.2 eV the total uncertainty in the measurement of W is on the order of 0.01 to 0.02. The presence of positive charge in the chamber was

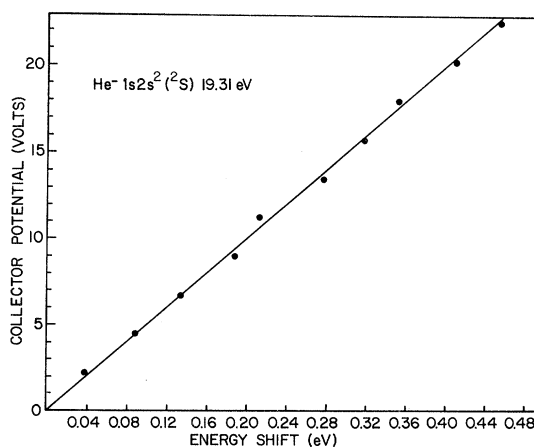


FIG. 2. Shift in the position of the 19.31-eV He transmission resonance as a function of the trapped-electron collector potential.

previously⁶ found to have no effect on the depth of the electron trapping well to any measurable extent since the positions of the He⁻(2s²2p) and He⁻(2s2p²) resonances observed in the positive-ion cross section are independent of pressure from 10⁻³ to 10⁻¹ Torr and electron-beam current from 10⁻¹⁰ to 10⁻⁸ Å.

The primary electron-energy scale was calibrated using the 19.31-eV transmission resonance and the 2³S peak in the He trapped-electron spectrum at 19.82 eV. The energy scale for Ne and Ar was established by using a mixture with helium. Energy scale determinations made using the He transmission resonance agree with measurements made by using the He²S peak in the excitation spectrum to within significantly less than 0.05 eV. Threshold excitation spectra were obtained with the automatic retarding potential-difference technique [full width of electron beam at half-height (FWHM) = 0.1–0.2 eV], and the cross-section measurements were recorded using a full beam width at half-maximum of 0.4–0.5 eV.

The cross section for producing an electron with energy less than or equal to W in an ionizing collision with an incident electron of energy E is given by

$$\sigma(E, W) = (1/Nl)(i_-/i_e), \quad (2)$$

where i_- is the trapped-electron current measured with a well depth W and an incident beam energy E , i_e is the transmitted electron-beam current, N is the number of target atoms per unit volume, and l is the ionization path length in the scattering chamber. In applying the expression above, care must be taken to ensure that the measurements are performed for values of N sufficiently small to ensure single-collision conditions. Since N is directly proportional to the pressure, this condition is satisfied if the ratio i_-/i_e is a linear function of pressure.

The quantity $\sigma(E, W)$ is an integral cross section and can be expressed as

$$\sigma(E, W) = \int_0^W \frac{d\sigma(E, \epsilon)}{d\epsilon} d\epsilon, \quad (3)$$

where $d\sigma(E, \epsilon)/d\epsilon$ represents the energy-differential cross section for producing an electron with energy between ϵ and $\epsilon + d\epsilon$ in an ionizing collision with an incident electron of energy E . In the definition of (3) we note that $d\sigma(E, \epsilon)$ results from integrating over all angular variables in the double-differential ionization cross section which is differential in both solid angle and energy.

In the present experiments, $\sigma(E, W)$ has been measured as a function of the maximum energy of the ejected electrons by keeping the incident beam energy constant and measuring the trapped-electron

current as a function of the well depth.

The maximum value of σ for incident energies below the second ionization potential is just twice the ionization cross section at the same incident energy. The maximum value is obtained with a well depth equal to the total kinetic energy of the emitted electrons. Under these conditions both of the final state electrons are trapped in the potential well, and the trapped-electron current is twice the positive-ion current. The energy distribution of the two electrons emitted in singly ionizing collisions is symmetric about the midpoint, owing to energy conservation. Consequently, for a well depth equal to half the kinetic energy available to the final-state electrons, σ will be equal to the ionization cross section.

The path length l in the present instrument is 4.12 cm. For those electrons in the beam whose velocity is not parallel to the magnetic field lines the path length will be increased owing to electron spiraling. The maximum increase in path length $(\Delta l)_{\max}$ for a nonaxial electron of energy E emerging from a slit of width d along a magnetic field of strength H is

$$(\Delta l)_{\max} = l \frac{1 - \{1 - 2.2 \times 10^{-4} (d^2 H^2 / E)\}^{1/2}}{\{1 - 2.2 \times 10^{-4} (d^2 H^2 / E)\}^{1/2}}, \quad (4)$$

where H is expressed in gauss, d in millimeters, and E in electron volts. The maximum increase is quite small (<10% increase) in the energy range employed in this work and was shown to be negligible since the measured cross sections were independent of magnetic field strength. This is taken as evidence that the velocities of most of the electrons are along the magnetic field lines. The gas density N is given by

$$N = 2.69 P(P/760)(273/T) \times 10^{19} \text{ cm}^{-3},$$

where P is the gas pressure in Torr, and T is the absolute temperature of the gas. We have assumed that the gas pressure is sufficiently low to allow the use of the ideal-gas law as the equation of state. T was determined by measuring the temperature of the scattering chamber. The pressure in the scattering chamber was measured with a Baratron capacitance manometer using a "1-Torr" pressure head.

Burrow and Schulz⁷ have discussed the effect of the increased path length of the elastically scattered electrons on the measurement of trapped-electron cross sections. At low-electron energy a fraction of the primary-electron beam is elastically scattered through large enough angles so that the axial component of velocity of the electrons is insufficient to escape the potential well at the ends of the trapped-electron chamber. An approximate expression was derived relating the true cross section and the measured cross section

assuming that the elastic scattering cross section is larger than the inelastic cross section and that the scattering is isotropic. Making these approximations, they obtained

$$\sigma_{\text{true}} = [1 - (W/E)^{1/2}] \sigma_{\text{measured}}, \quad (5)$$

where W is the well depth and E is the incident electron energy.

In the present study the maximum correction to our data is when $W=0.9$ eV and $E=30$ eV, which amounts to a calculated 17% correction factor. The elastic scattering, however, in the rare gases at high energy is highly forward collimated (see Ref. 8, pp. 334, 335). Thus the real correction to be applied to our data is less than 5%. Owing to the smallness of this correction, we have not attempted to further refine the treatment of Ref. 7 to include the fact that the elastic scattering cross section is peaked in the forward direction.

A possible source of error in the present measurements of absolute slow-electron-production cross sections can be that due to stray electron current collected from secondary electrons produced by metastable helium atoms striking the wire grid which is used to define the electron trap volume. The wire grid is 97% transmitting so that only 3% of the metastable helium formed in the beam can be effective in producing a contribution to the slow-electron current. From the cross-section measurements of Fleming and Higginson,⁹ the maximum contribution would occur for incident electrons of about 30 eV. This contribution is expected to increase the measured cross section by only 1×10^{-19} cm² for helium. The correction becomes smaller at higher and lower incident electron energies. Again only those electrons whose energy falls within the well depth or whose velocity component perpendicular to the magnetic field axis is insufficient to escape the ends of the tube will be collected, and thus the contribution is expected to be significantly less than 10^{-19} cm². Additional evidence that this correction to our measured cross sections is negligible comes from the fact that the shape of the trapped-electron current below the ionization threshold does not show the characteristic features of metastable-helium production seen previously (see Ref. 8, p. 254).

In order to check the experimental apparatus for systematic errors, the total-ionization cross sections for He, Ne, and Ar were measured from the ionization threshold to 150 eV. The total-ionization cross section σ_T is related to the individual cross sections $\sigma_1, \sigma_2, \sigma_3, \dots$ for single, double, triple, . . . ionization by

$$\sigma_T = \sigma_1 + 2\sigma_2 + 3\sigma_3 + \dots$$

The total-ionization cross section could be reproducibly measured from month to month to within

$\pm 5\%$. Most of the previous studies cited have given error estimates no larger than $\pm 5\%$, but such estimates were also derived from the reproducibility of the measured values under the experimental conditions used to perform the measurements, as noted by Kieffer and Dunn.¹⁰ Consequently, such estimates are not reliable indications of the systematic errors involved in the measurements, since these must be assessed independently.

A better indication of the systematic errors is obtained by studying Table I which compares the cross sections measured in the present study at 100 eV to those reported by other experimenters. Deviations between the present measurements and those of others as large as $\pm 15\%$ are frequent in the tabulated ratios. The present measurements are consistently below the values obtained by Tozer and Craggs,¹¹ Asundi and Kurepa,¹² and Smith¹³ but never by a constant amount in any of the three cases. The present measurements range from 13% below the measurements of Rapp and Englander-Golden¹⁴ for He to 21% above for Ar. Except for Ar, where the disagreement is 26%, the present measurements agree most closely with the values measured by Schram and co-workers¹⁵ at 100 eV. The cross-section measurements presented here are for comparison purposes only and no claim for better accuracy over previous work is made.

It is difficult to accurately assess error limits in the present measurements of absolute cross sections for production of slow electrons. The errors due to increased path length resulting from spiraling and due to the collection of secondary electrons produced by metastable helium striking the grid wire are in the direction to overestimate the integral cross sections. However, we argue that these errors are less than 5%. Uncertainty in the well depth (± 0.02 eV) introduces an error in the integral cross section of approximately $\pm 10\%$. The contribution of systematic errors is estimated to be $\pm 15\%$. This number is arrived at by consideration of errors in measurements of pressure, geometric path length, and current measurements along with comparison of our positive-ion cross-section measurements with others in Table I. Thus the limits of error in the present cross-section

TABLE I. Ratios of ionization cross sections at 100 eV measured in the present work to those reported by other experimenters.

Gas	Smith (Ref. 13)	Rapp (Ref. 14)	Schram (Ref. 15)	Asundi (Ref. 12)	Tozer (Ref. 11)
He	0.89	0.87	0.98	0.83	
Ne	0.86	0.96	1.01	0.84	
Ar	0.95	1.21	1.26		0.96
Kr		1.11	1.06	0.87	0.91
Xe		1.18	1.03	0.81	0.81

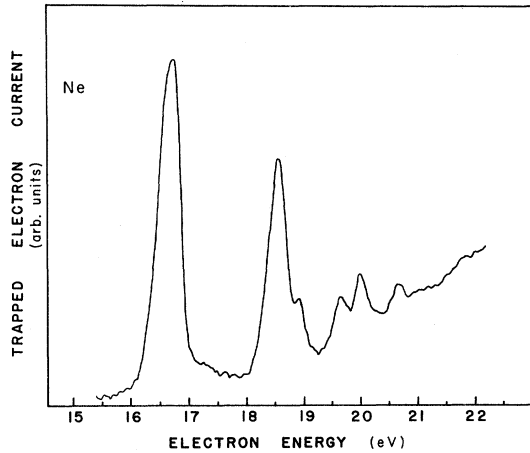


FIG. 3. Trapped-electron excitation spectrum of neon. Well depth is 0.13 eV and the pressure is 1.5×10^{-2} mm Hg.

measurements are assessed to be +30, -25%.

A. Threshold Excitation Spectra of Ne and Ar

Trapped-electron excitation spectra of He have been exhaustively studied in the energy region below the first-ionization threshold.⁴ For completeness we present trapped-electron studies of the excited states of Ne and Ar below the ionization potential.

The Ne threshold electron excitation spectrum below the ionization limit is shown in Fig. 3, measured using the automatic retarding-potential-difference (RPD) technique with a gas pressure of 1.5×10^{-2} Torr and a well-depth energy of 0.13 eV. The total resolution is approximately 0.15 eV (FWHM). The energies of the peaks were mea-

TABLE II. Threshold excitation spectrum of neon below the ionization threshold.

Measured values		Spectroscopic data (Ref. 16)			
Energy (eV)	Deviation (eV)	Configuration	Designation	J	Energy (eV)
		$2p^6$	$2p^6 1S$	0	0
		$2p^5(^2P_{3/2}^0)3s$	$3s[\frac{3}{2}]^0$	1	16.67
16.74	0.02	$2p^5(^2P_{1/2}^0)3s$	$3s[\frac{1}{2}]^0$	0	16.71
		$2p^5(^2P_{3/2}^0)3p$	$3p[\frac{3}{2}]$	3	18.55
18.56	0.02			2	18.57
		$2p^5(^2P_{3/2}^0)3p$	$3p[\frac{3}{2}]$	1	18.61
				2	18.64
		$2p^5(^2P_{1/2}^0)3p$	$3p[\frac{1}{2}]$	1	18.73
18.89	0.02			0	18.97
		$2p^5(^2P_{3/2}^0)4s$	$4s[\frac{3}{2}]$	2	19.66
19.67	0.04			1	19.69
		$2p^5(^2P_{1/2}^0)4s$	$4s[\frac{1}{2}]^0$	0	19.76
		$2p^5(^2P_{3/2}^0)3d$	$3d[\frac{3}{2}]^0$	0	20.02
20.02	0.02			0	20.02
20.20	0.05	$2p^5(^2P_{3/2}^0)4p$	$4p[\frac{3}{2}]$	0	20.26
20.67	0.02	$2p^5(^2P_{1/2}^0)5s$	$5s[\frac{1}{2}]^0$	0	20.66

TABLE III. Threshold excitation spectrum of argon below the ionization threshold.

Measured values		Spectroscopic data (Ref. 16)			
Energy (eV)	Deviation (eV)	Configuration	Designation	J	Energy (eV)
		$3p^6$	$3p^6 1S$	0	0
11.55	0.03	$3p^5(^2P_{3/2}^0)4s$	$4s[\frac{3}{2}]^0$	2	11.55
				1	11.62
11.7	0.04	$3p^5(^2P_{1/2}^0)4s$	$4s[\frac{1}{2}]$	0	11.72
12.91	0.02	$3p^5(^2P_{3/2}^0)4p$	$4p[\frac{3}{2}]$	1	12.91
		$3p^5(^2P_{3/2}^0)4p$	$4p[\frac{3}{2}]$	3	13.07
13.10	0.02			2	13.09
		$3p^5(^2P_{3/2}^0)4p$	$4p[\frac{3}{2}]$	1	13.15
				2	13.17
14.07	0.02	$3p^5(^2P_{3/2}^0)5s$	$5s[\frac{3}{2}]$	2	14.07
				1	14.09

sured with respect to the He 2^3S level and 19.31-eV transmission resonance using a mixture of He and Ne. The results of these measurements are shown in Table II along with spectroscopic data giving the configurations and energies of the peaks in the spectrum. Again, the quoted energy deviations represent only the standard deviations in the average energy values of all the measurements performed and do not necessarily correspond to the actual errors in the absolute energy measurements.

Note that the levels of Ne do not obey LS coupling but are designated according to the jl coupling scheme used by Moore.¹⁶ The spectrum of Ne is sufficiently complex that quite often the peaks in the trapped-electron spectrum could be identified with more than one possible level, as shown in Table II. In choosing the levels shown, the criterion of selecting states having the lowest possible total angular momentum J was used when other factors were equal. This guideline is based on the fact that for a zero energy outgoing electron the value of J must represent the total angular momentum of the incident electron, since the Ne ground state has $J=0$, and to first order the lower angular momentum incoming waves might be expected to contribute more strongly to the inelastic collisions. It can be argued on the basis of the data that this assumption seems justified for all of the levels seen in Ne to within the resolution of the present measurements.

Figure 4 illustrates results for the threshold excitation spectrum of Ar below the ionization threshold at 15.8 eV. Measurements were made using the RPD technique at a pressure of 5×10^{-3} Torr and with a well-depth energy of approximately 0.13 eV. The energies of the four features common to all of the Ar excitation spectra recorded are given in Table III. Also shown are the standard deviations in the averages of all the measure-

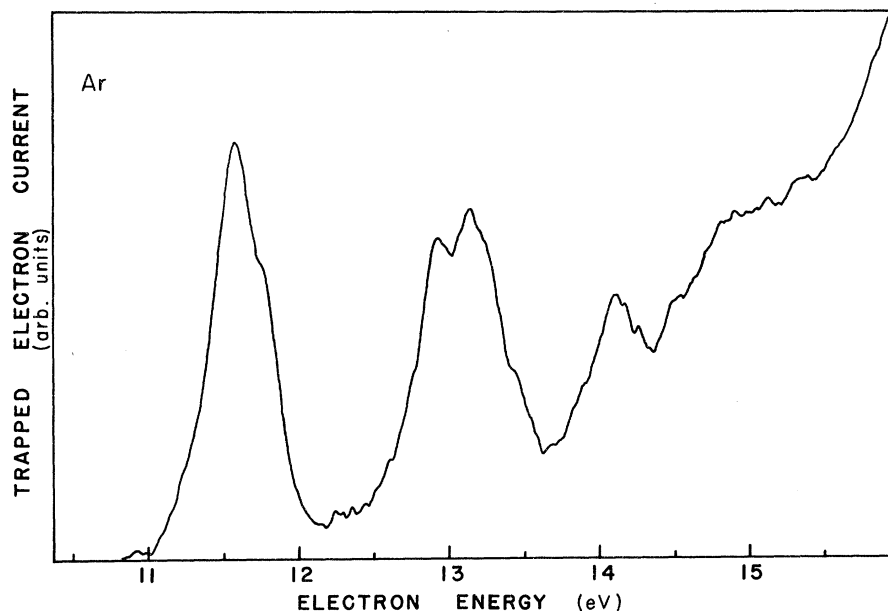


FIG. 4. Trapped-electron excitation spectrum of argon. Well depth is 0.13 eV and the pressure is 5×10^{-3} mm Hg.

ments performed along with the configurations and energies of some of the Ar energy levels derived from spectroscopic data which correspond in energy to the observed peaks. Note the excellent agreement between the measured energies and the spectroscopic levels. The levels in the Ar spectrum obey jl coupling as shown. It is interesting to note that the peaks in the threshold spectrum correlate with levels having J values greater than zero. This requires that the incident or exit angular momentum state of the projectile be greater

than zero since the angular momentum of the Ar ground state is $J=0$. The only exception is the shoulder at 11.7 eV on the high-energy side of the first peak which appears to be the state at 11.72 eV with $J=0$.

The threshold excitation spectra for Ne and Ar may be compared with analogous spectra obtained by Brion and Olsen¹⁷ through utilization of the SF_6 scavenger technique.¹⁸ In these experiments the ability of SF_6 to capture very slow electrons (energies < 0.05 eV) was used to detect slow electrons

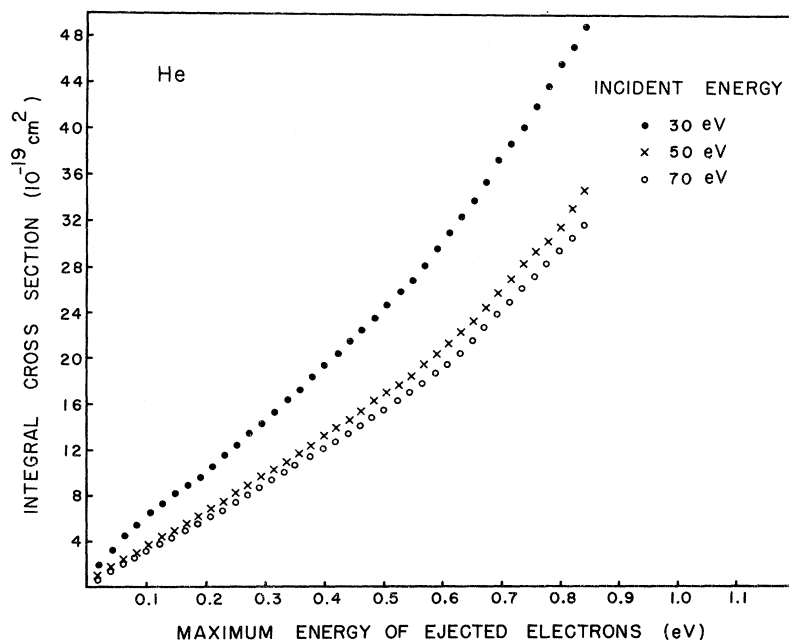


FIG. 5. He trapped-electron cross sections as a function of the potential-well energy.

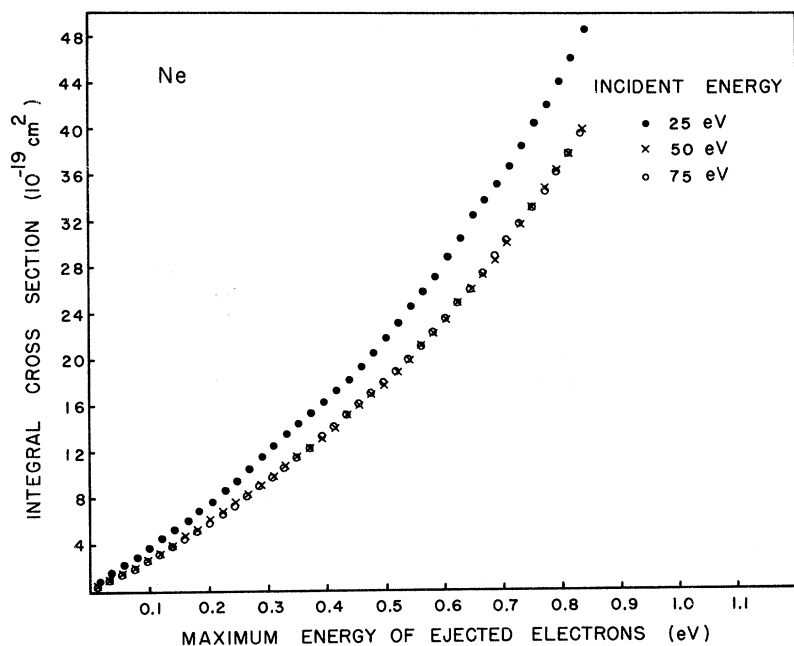


FIG. 6. Ne trapped-electron cross sections as a function of the depth of the potential well. The maximum energy of the ejected electrons is taken to be the depth of the potential well.

resulting from excitation and ionization of noble gases. The spectra below the ionization potential are very similar to those presented in the present trapped-electron experiment. However, the results differ significantly in the region above the ionization threshold as will be discussed below.

B. Slow-Electron Production Cross Sections

The results of the slow-electron integral-cross-section measurements are shown for He, Ne, and

Ar in Figs. 5-7, respectively. The measurements were performed by keeping the incident electron-beam energy fixed and measuring the trapped-electron current as a function of the well depth which represents the maximum energy of the collected electrons. In order to maintain constant electron energy, the accelerating voltage had to be adjusted each time the well depth was changed. The incident beam energies were chosen in each case to coincide with regions in which the trapped-

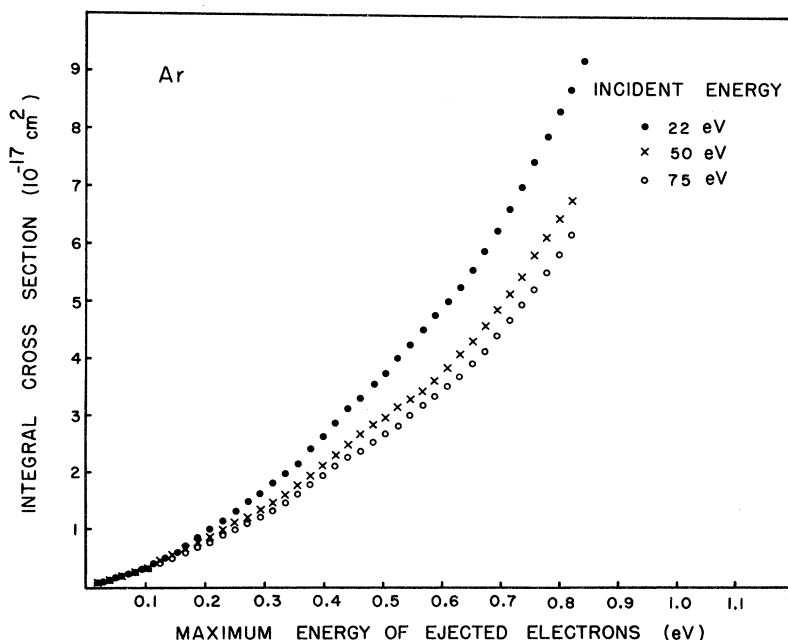


FIG. 7. Ar trapped-electron cross sections as a function of the depth of the potential well. The maximum energy of the ejected electrons is taken to be the depth of the potential well.

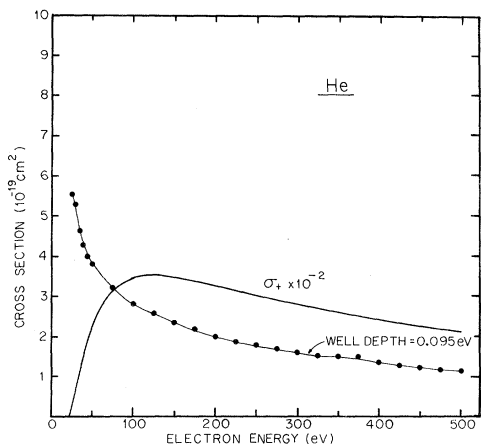


FIG. 8. Cross section for production of secondary electrons from 0 to 0.095 eV as a function of the incident electron energy for He. The solid curve is the positive-ionization cross section taken from Rapp and Englander-Golden (Ref. 14).

electron spectra are relatively constant, so that fluctuations in the incident beam energy would have a minimal effect on the final results. The cross sections shown illustrate the slow variations in the trapped-electron spectra over a broad energy range for a constant value of the well-depth energy.

The cross sections for producing electrons in the energy range from 0 to 0.095 eV are shown for He, Ne, and Ar in Figs. 8–10, respectively, for incident electron energies from the ionization threshold to ~ 500 eV. Included in the figures are the ionization cross-sections curves of Rapp and Englander-Golden.¹⁴

We note that the integral cross sections $\sigma(E, W)$ of Figs. 8–10 exhibit an energy dependence which is quite different from that of the total-ionization cross sections at low incident energies ($E < 200$ eV) but quite similar at high energies. The cross sections for producing electrons with energies from 0 to W bear a closer resemblance to inelastic scattering cross sections for excitations to excited Rydberg states of the target atom than to the corresponding total-ionization cross sections. The peak in $\sigma(E, W)$ occurs at an energy much lower than the corresponding maximum in the total-ionization cross section. This is shown in Fig. 11 which is a plot of the lower-energy portion of $\sigma(E, W)$ for He with a value of $W = 0.42$ eV. The maximum in Fig. 11 occurs at about 30 eV, whereas the total-ionization cross section peaks at about 120 eV. If one examines the total inelastic scattering cross sections of St. John, Miller, and Lin¹⁹ for transitions $1S \rightarrow n^{1,3}L$ for He, the similarity to the integral cross section $d\sigma(E, W)$ of Fig. 8 is much greater than that between $d\sigma(E, W)$ and the

total-ionization cross section. This behavior is easily understood by the following argument.

In the present experiment we observe those excitations into the continuum in which one of the electrons has a very small amount of energy, and the second electron carries off essentially all the energy in excess of that necessary for ionization. Thus, in the transitions involved here the low-energy electron moves in the ionic field of the target in a state which is barely in the continuum. Of course, the wave functions for very low-positive-energy states of the ion are practically indistinguishable from those for very high Rydberg states of the atom. Thus, the excitation functions for high Rydberg states should go smoothly into the continuum if one observed a transition $1^1S \rightarrow \epsilon^{1,3}L$, where the energy $\epsilon \sim 0$. The present cross sections represent an integral over such continuum states from $\epsilon = 0$ to $\epsilon = W$ and a sum over all the S, P, D , etc., angular momentum contribution for the outgoing electron. Thus, the cross sections for ionization in which one of the slow electrons is barely in the continuum should look very similar to an average of the excitation cross sections for high Rydberg levels of the target. The cross sections $\sigma(E, W)$ do, in fact, have this general character with a maximum at around 30 eV and a decrease at large energy which closely approximates the $(1/E) \ln E$ form for allowed transitions.

The preceding argument was verified numerically for the case of collisional ionization of hydrogen where the Born-approximation results are available in analytical form. Integral ionization cross sections $\sigma(E, W)$ were obtained for various well depths W and compared with the total-ionization and with inelastic-collision cross sections as

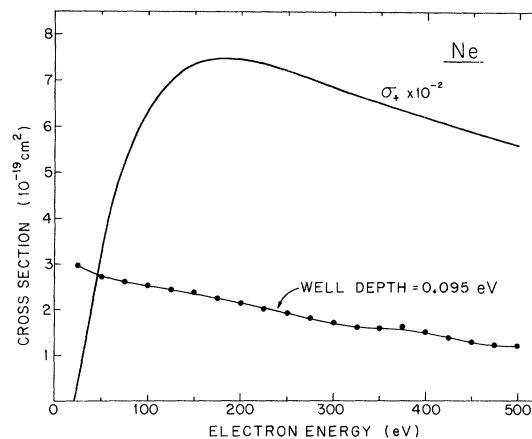


FIG. 9. Cross section for production of secondary electrons from 0 to 0.095 eV as a function of the incident electron energy for Ne. The solid curve is the positive-ionization cross section taken from Rapp and Englander-Golden (Ref. 14).

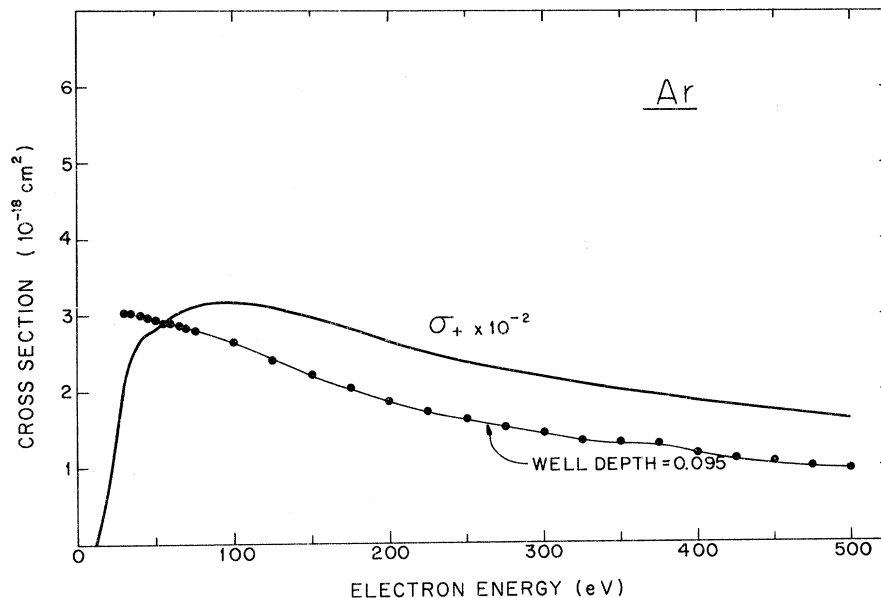


FIG. 10. Cross section for production of secondary electrons from 0 to 0.095 eV as a function of the incident electron energy for Ar. The solid curve is the positive-ionization cross section taken from Rapp and Englander-Golden (Ref. 14).

shown in Fig. 12. The behavior is similar to that observed experimentally for the noble gases He, Ne, and Ar.

As mentioned above, Brion and Olsen¹⁷ obtained slow-electron production spectra for the noble gases in the region immediately above the ionization threshold. Their SF₆ scavenger data show a much more rapid increase in the number of slow electrons produced in the first few volts immediately above the ionization threshold than is the case with the present data. They obtained a rate of increase which agreed approximately with a prediction of Temkin,²⁰ namely, that the yield of zero-energy electrons in the energy region immediately above threshold should go as the excess energy to the 0.5 power. The present results do not show such a rapid increase in yield and agree more closely with the prediction of Wannier²¹ and, more recently, of Rau²² who predicted that the increase should be proportional to the 0.127 power of the energy in excess of that necessary to ionize the target. However, in the present experiment all electrons with energies from 0 to 0.10 eV (well depth equal to 0.1 eV) were detected. Thus, no direct comparison with the theory of Wannier²¹ or Rau²² is possible.

It should be mentioned that chemi-ionizing collisions between highly excited Rydberg states and SF₆ (i. e., He^{**} + SF₆ → He⁺ + SF₆⁻) are known²³ to proceed with large cross sections (~10⁻¹² cm²) and will undoubtedly contribute to the SF₆⁻ signal above the ionization threshold. This effect undoubtedly is partly responsible for the differences in shape between the trapped-electron and the scavenger spectra.

Quite recently, Opal, Peterson, and Beaty² have reported measurements of energy and angular distributions of electrons ejected from helium for incident electron energies between 100 and 2000 eV. The secondary-electron energy spectra were normalized by using the previously measured electron scattering cross sections of Williams,²⁴ and the angular distributions were integrated over angle to give secondary-electron energy distributions. It was necessary to linearly extend the measurements to smaller and larger angles to perform the integration. Figure 13 shows a comparison of the present measurements at low-secondary-electron energies (<1 eV) for a primary-electron energy of 100 eV. Also shown are the Born and the Born-exchange calculations of Sloan.²⁵ The latter calcu-

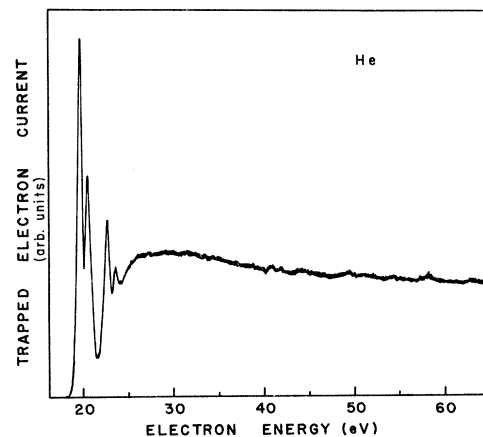


FIG. 11. Low-energy portion of the integral cross section for He. Well depth = 0.42 eV.

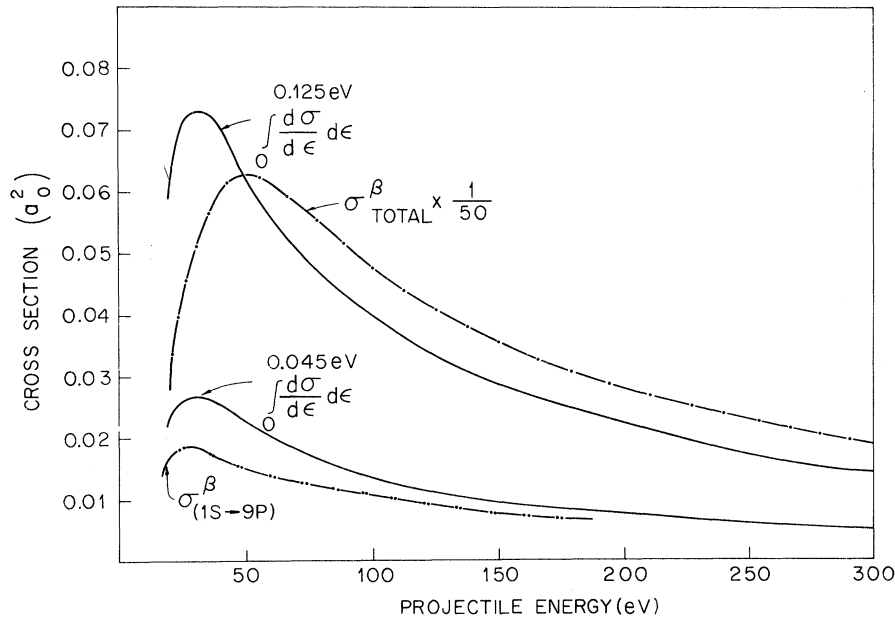


FIG. 12. Born cross sections for production of electrons with energies from zero to W in ionization of hydrogen (solid line); corresponding Born result for total-ionization cross section (dot-dashed line); Born cross section for excitation of $1S \rightarrow 9P$ state in hydrogen (double-dot-dashed line).

lations were normalized at an ejected electron energy of 14 eV.

It is to be noticed that the Born-exchange approximation calculations fall exactly upon the present low-energy secondary-electron cross sections if the high-energy secondary-electron measurements of Opal, Peterson, and Beaty² are used to normalize the calculations. There is a noticeable

deviation of the low-energy measurements of Ref. 2; however, in general there is excellent agreement between the two measurements and the shape of the energy distributions provided by theory.

Finally, in a recent paper, Omidvar, Kyle, and Sullivan²⁶ have calculated differential cross sections for ionization for a number of atomic species including helium and neon, both of which can be compared to the present experiment. These authors employed the Born approximation and assumed the active atomic electron to be in a Coulomb field. The active electron was described before ejection by a Coulomb function with an effective charge chosen such that the mean radius would

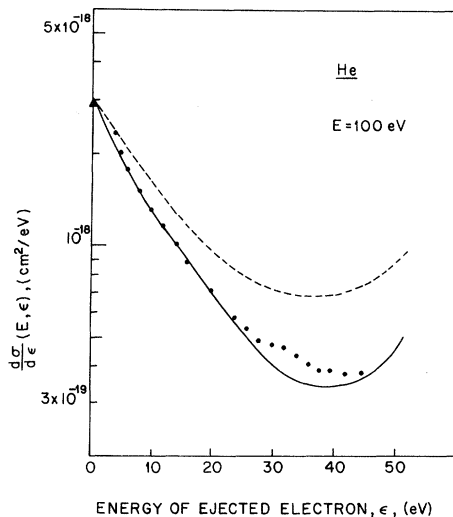


FIG. 13. Secondary-electron energy distribution produced by 100-eV primary electrons on helium: Born (dashed line); Born-exchange calculation of Sloan (Ref. 25) (solid line); results of Opal, Peterson, and Beaty (Ref. 2) (dotted line); present result (Δ). The calculations are normalized to the experiment of Opal, Peterson, and Beaty at a secondary-electron energy of 14 eV.

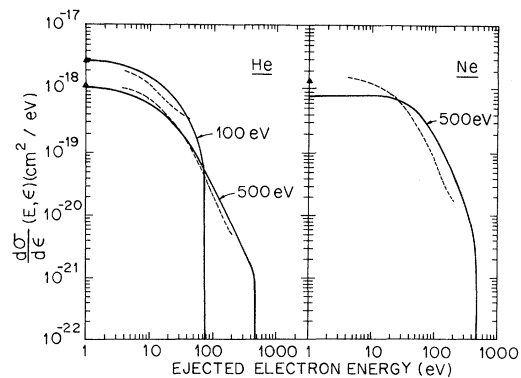


FIG. 14. Secondary-electron energy distribution produced by 500-eV primary electrons: Born calculation of Omidvar, Kyle, and Sullivan (Ref. 26) (solid line); data of Opal, Peterson, and Beaty (Ref. 2) (dotted line); present result (Δ). The calculations of Omidvar, Kyle, and Sullivan are absolute.

agree with that from a Hartree-Fock treatment of the target system. Their calculated cross sections for ejection of secondary electrons for incident electrons of 100 and 500 eV on He are in reasonable agreement with the measurements of Opal, Peterson and Beaty² and agree exactly with the present low-energy trapped-electron data. Figure 14 compares the theory of Omidvar, Kyle, and Sullivan²⁸ with the measurements of Opal, Peterson, and Beaty and the present results for neon. The

low-energy distributions ($\epsilon < 20$ eV) calculated by Omidvar, Kyle, and Sullivan are seen to be somewhat flatter than those shown in the measurements of Opal, Peterson and Beaty and fall below the low-energy datum point obtained in the present experiment for 500-eV incident electrons on neon.

ACKNOWLEDGMENT

The authors are indebted to P. D. Burrow for many helpful comments.

†Research sponsored by the U. S. Atomic Energy Commission under contract with Union Carbide Corporation.

*Present address: Sandia Laboratories, P. O. Box 5800, Albuquerque, N. M. 87115.

¹H. Ehrhardt, M. Schulz, T. Tekaas, and K. Willman, *Phys. Rev. Letters* **22**, 89 (1969).

²C. B. Opal, W. K. Peterson, and E. C. Beaty, *J. Phys. B* **4**, 1020 (1971); W. K. Peterson, E. C. Beaty, and C. B. Opal, *Phys. Rev. A* **5**, 712 (1972).

³R. N. Compton, J. A. Stockdale, and P. W. Reinhardt, *Phys. Rev.* **180**, 111 (1969).

⁴G. J. Schulz, *Phys. Rev.* **112**, 150 (1958).

⁵C. E. Kuyatt, J. A. Simpson, and S. R. Mielczarek, *Phys. Rev.* **138**, A385 (1965).

⁶J. T. Grissom, R. N. Compton, and W. R. Garrett, *Phys. Letters* **30A**, 117 (1969).

⁷P. D. Burrow and G. J. Schulz, *Phys. Rev.* **187**, 97 (1969).

⁸H. S. W. Massey and E. H. S. Burhop, *Electronic and Ionic Impact Phenomena* (Oxford U. P., London, 1969), Vol. 1.

⁹R. J. Fleming and G. S. Higginson, *Proc. Phys. Soc. (London)* **84**, 531 (1964).

¹⁰L. J. Kieffer and G. H. Dunn, *Rev. Mod. Phys.* **38**, 1 (1966).

¹¹B. A. Tozer and J. D. Craggs, *J. Electron. Control* **8**, 103 (1960).

¹²R. K. Asundi and M. V. Kurepa, *J. Electron. Control* **15**, 41 (1963).

¹³P. T. Smith, *Phys. Rev.* **36**, 1293 (1930); **37**, 808 (1931).

¹⁴D. Rapp and P. Englander-Golden, *J. Chem. Phys.* **43**, 1464 (1965).

¹⁵B. L. Schram, F. J. de Heer, M. J. van der Wiel, and J. Kistemaker, *Physica* **31**, 94 (1965); B. L. Schram, H. R. Moustafa, J. Schutten, and F. J. de Heer, *ibid.* **32**, 734 (1966).

¹⁶C. E. Moore, *Atomic Energy Levels*, Nat. Bur. Std. Publ. (U. S. GPO, Washington, D. C., 1948).

¹⁷C. E. Brion and L. A. R. Olsen, *J. Phys. B* **3**, 1020 (1970).

¹⁸For reference to the SF₆ scavenger technique, see R. K. Curran, *J. Chem. Phys.* **38**, 780 (1963); R. N. Compton and R. H. Huebner, in *Advances in Radiation Chemistry*, edited by M. Burton and J. L. Magee (Wiley-Interscience, New York, 1970), Vol. 2.

¹⁹R. M. St. John, F. L. Miller, and C. C. Lin, *Phys. Rev.* **134**, A888 (1964).

²⁰A. Temkin, in *Physics of the One- and Two-Electron Atoms*, edited by F. Bopp and H. Keimpoppen (North-Holland, Amsterdam, 1969), p. 655.

²¹G. H. Wannier, *Phys. Rev.* **90**, 817 (1953).

²²A. R. P. Rau, *Phys. Rev. A* **4**, 20 (1971).

²³H. Hotop and A. Niehaus, *J. Chem. Phys.* **47**, 2506 (1967).

²⁴K. L. Williams, in *Abstracts of Sixth International Conference on the Physics of Electronic and Atomic Collisions* (MIT Press, Cambridge, Mass., 1969), pp. 735-737.

²⁵I. H. Sloan, *Proc. Phys. Soc. (London)* **85**, 435 (1965).

²⁶K. Omidvar, H. L. Kyle, and E. C. Sullivan, *Phys. Rev. A* **5**, 1174 (1972).